Influence of IV Contrast Administration on CT Measures of Muscle and Bone Attenuation: Implications for Sarcopenia and Osteoporosis Evaluation

Robert D. Boutin[1]
Justin M. Kaptuch[1]
Cyrus P. Bateni[1]
James S. Chalfant[1]
Lawrence Yao[2]

OBJECTIVE. The objective of our study was to characterize enhancement of muscle and bone that occurs on standardized four-phase contrast-enhanced CT.

MATERIALS AND METHODS. Two musculoskeletal radiologists reviewed standardized four-phase abdominal CT scans obtained with IV contrast material. The psoas area was measured, and the mean attenuation (in Hounsfield units) was recorded for the aorta, psoas muscles, posterior paraspinal muscles, and L4 vertebral body. CT attenuation measures were compared between anatomic regions and imaging phases with the paired *t* test; associations between measures were examined with the Pearson correlation coefficient (*R*).

RESULTS. The study included 201 patients (97 men, 104 women; mean age, 57.7 ± 12.5 [SD] years). Subject age was inversely correlated with unenhanced attenuation in the psoas muscles, posterior paraspinal muscles, and L4 ($p < 0.001$). The psoas muscles, posterior paraspinal muscles, and L4 enhanced significantly ($p < 0.001$) at all three contrast-enhanced phases. The greatest muscle enhancement was observed on delayed phase scans, whereas the greatest enhancement in L4 was seen on portal phase imaging. The unenhanced attenuation of the psoas muscles was significantly and negatively correlated with enhancement of the psoas muscles at the portal and delayed phases ($p < 0.05$ and $p < 0.01$, respectively), but these correlations were not seen for the posterior paraspinal muscles. Age was positively correlated with posterior paraspinal muscle enhancement at the portal and delayed phases in men ($p < 0.05$ and $p < 0.01$, respectively) but not in women.

CONCLUSION. Contrast enhancement of commonly measured muscle and bone regions is routinely observed and should be considered when using CT attenuation values as biomarkers of sarcopenia and osteoporosis. Furthermore, CT enhancement may be significantly influenced by age, sex, and unenhanced tissue attenuation.

Keywords: contrast media, CT, osteoporosis, sarcopenia, skeletal muscle

DOI:10.2214/AJR.16.16387

Received March 10, 2016; accepted after revision April 30, 2016.

The opinions and assertions contained herein are the private views of the authors and are not to be construed as official or as representing the views of the National Institutes of Health.

Based on a presentation at the 2016 Society of Skeletal Radiology annual meeting, New Orleans, LA.

[1]Department of Radiology, University of California Davis School of Medicine, 4860 Y St, Ste 3100, Sacramento, CA 95817. Address correspondence to R. D. Boutin (rdboutin@ucdavis.edu).

[2]Department of Radiology and Imaging Sciences, National Institutes of Health, Bethesda, MD.

This article is available for credit.

AJR 2016; 207:1046–1054

0361–803X/16/2075–1046

Just as so-called "phantomless" clinical CT is now used to quantitate bone mineral density for the diagnosis of osteoporosis [1–4], CT is increasingly being used to quantitate skeletal muscle attenuation for the diagnosis of sarcopenia (i.e., muscle depletion) [5, 6]. Low muscle attenuation on CT generally is attributed to myosteatosis (i.e., fatty infiltration of muscle) [7]. Myosteatosis is associated with adverse outcomes, including decreased strength and mobility, systemic metabolic abnormalities (e.g., diabetes, obesity), postoperative complications [8], and increased mortality [9–13]. Given the recently discovered roles of muscle as an endocrine organ [14, 15], other systemic effects of myosteatosis have also been suggested, including a possible association with hepatic steatosis [16–18].

Although low muscle attenuation on CT is now regarded as a negative prognostic factor in patients with cancer and other conditions, numerous studies have measured muscle attenuation or "lean muscle" without differentiating between CT examinations performed with versus without IV contrast material [8, 9, 13, 19–26]. We wondered whether IV contrast administration should be accounted for when using tissue attenuation measurements as biomarkers. To our knowledge, the potential effects of IV contrast material on CT attenuation–based criteria used to diagnose myosteatosis have not been systematically examined.

Opportunistic measurements of both bone and muscle attenuations have been proposed as useful, readily accessible biomarkers for osteoporosis and sarcopenia. IV contrast material may significantly affect CT mea-

surements of bone mineral density [27–29], although some authors have found that contrast-enhanced CT is equivalent to unenhanced CT for opportunistic osteoporosis screening [30]. In a recent position statement, the International Society for Clinical Densitometry [31] concluded that "there is insufficient evidence to judge the effect of contrast agents" on CT-measured bone mineral density in part because it must first be determined whether the presence and timing of contrast administration are significant.

Regarding muscle enhancement, an early study from an era before automated contrast material injection reported no consistent increase in muscle attenuation on contrast-enhanced CT [32]. However, there have been numerous technologic advances in CT [33] and extensive contrast media research in recent decades [34]. To date, the enhancement characteristics of muscle with the use of current multiphase contrast-enhanced CT protocols are not well documented. If muscle or bone enhancement is sufficiently consistent, then CT attenuation measurements performed after IV administration of contrast material might be amenable to empiric correction.

We hypothesized that IV contrast material significantly increases the CT attenuation of both muscle and bone. Our primary study aim was to document the changes in paravertebral core muscle attenuation that occur during the arterial, portal, and delayed phases after IV contrast injection compared with unenhanced images and to clarify the implications for applying CT attenuation–based markers to evaluate sarcopenia and osteoporosis. Our secondary aim was to examine potential associations between muscle or marrow enhancement and other patient and CT features (e.g., age, sex, body mass index [BMI], two proposed CT biomarkers of sarcopenia). Finally, because of recently described linkages between sarcopenia and hepatic steatosis, we included a marker of hepatic steatosis in our analysis.

Materials and Methods

Patients and Study Design

After obtaining institutional review board approval with a waiver of informed consent, we performed a retrospective study at a single hospital of patients who met three inclusion criteria. The first criterion was age of 18 years old or older. The second criterion was availability of the following clinical data obtained within 6 months of the CT examination: age, sex, height, weight, history of diabetes mellitus, history of liver disease, serum creatinine value, serum bilirubin value, international normalized ratio, and model for end-stage liver disease (MELD) score for chronic liver disease severity calculated from the latter three values. The third criterion was a diagnostic four-

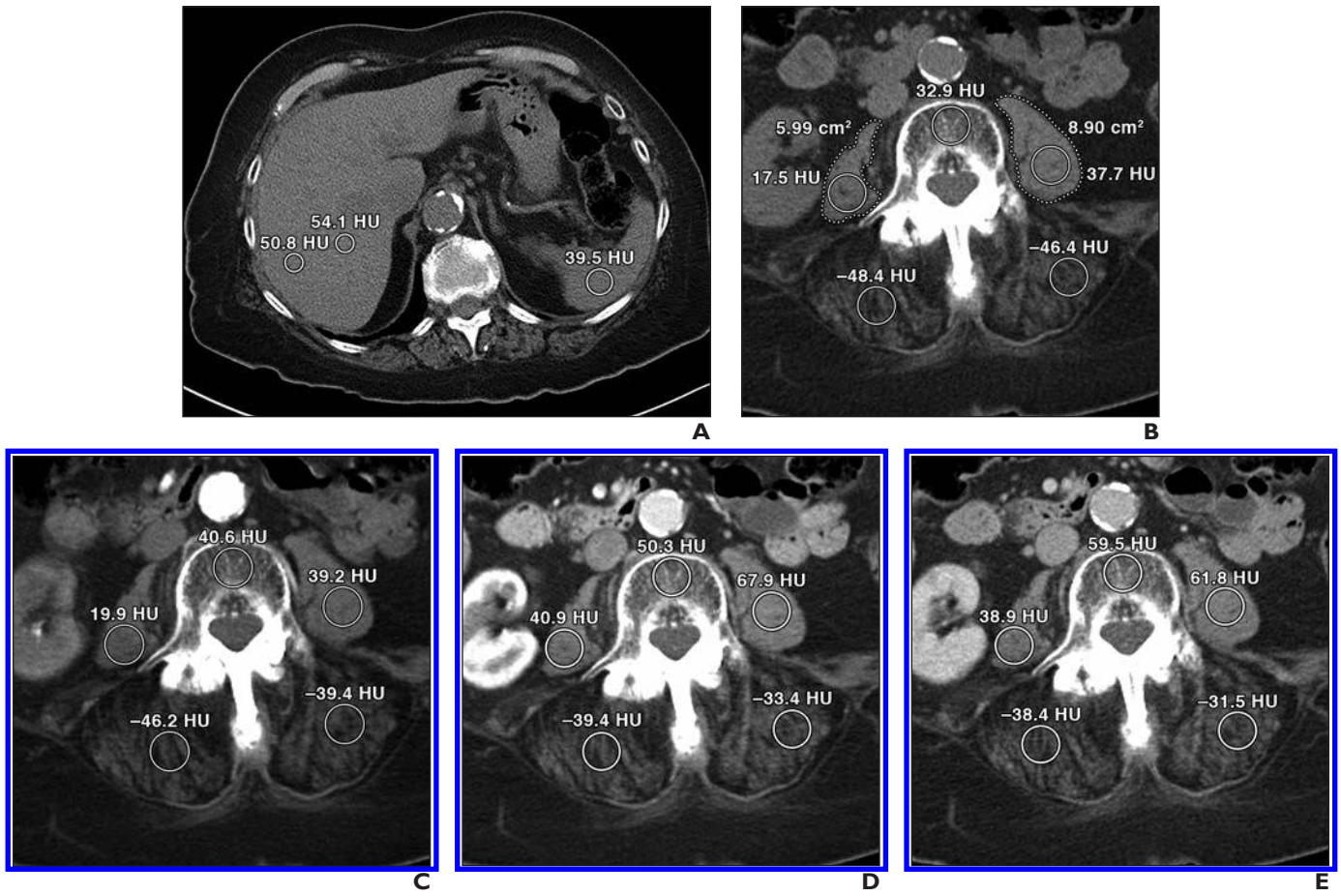

Fig. 1—88-year-old woman with right upper quadrant and back pain.
A, Unenhanced CT scan shows representative ROIs (*circles*) for liver and spleen before administration of contrast material.
B–E, Representative four-phase CT scans obtained in unenhanced phase (**B**), arterial phase (**C**), portal phase (**D**), and delayed phase (**E**) show ROIs (*circles*) for psoas muscles, posterior paraspinal muscles, and L4 vertebral body. For example, attenuation of L4 vertebral body increased from 32.9 HU in unenhanced phase to 40.6 HU in arterial phase, 50.3 HU in portal phase, and 59.5 HU in delayed phase. Attenuation of abdominal aorta also was measured on each of four phases of CT examination at L3 level above level of aortic bifurcation (not shown). In **B**, dotted lines show freehand ROIs drawn on unenhanced images outlining both psoas muscles.

phase abdominal CT examination that covered the L3 and L4 levels and was performed during evaluation for abdominal disorders with IV injection of 125 mL of iohexol containing 350 mg I/mL administered at an injection rate of 4 mL/s. Although no patients met our predefined exclusion criteria, patients were to be excluded if records indicated that they belonged to a predefined vulnerable population (i.e., pregnant, imprisoned, or cognitively impaired patients) or if metallic artifact (e.g., spinal instrumentation) at the L3 or L4 level was observed by either of the two readers. Two hundred one consecutively selected patients met the inclusion criteria between September 18, 2010, and September 3, 2015.

CT Examination Protocol

Patients were centered within the CT gantry (using a laser light guide) in a supine feet-first position. CT examinations were performed in the helical mode without gantry tilt on five MDCT scanners: four 64-MDCT scanners (one Somatom Definition, Siemens Healthcare; one Somatom Sensation, Siemens Healthcare; two LightSpeed VCT, GE Healthcare) and one 128-MDCT scanner (Somatom Definition AS+, Siemens Healthcare). Daily calibration of the CT scanners was completed using manufacturer-supplied phantoms to ensure consistency in attenuation measurements in accordance with manufacturer specifications. Scans were obtained at 120 kV with a gantry rotation speed of 0.5 or 0.6 second. Scanning was conducted with automated dose modulation (e.g., reference effective tube current of 220–260 mA using an automatic exposure control technique [CARE Dose4D, Siemens Healthcare]). Beam collimation ranged from 20 to 40 mm, and all ROI measurements were made on 5-mm-thick axial images reconstructed using a filtered backprojection technique with the standard body filter (on GE Healthcare scanners) or a B40f kernel (on Siemens Healthcare scanners).

CT studies with multiple contrast-enhanced phases were performed to provide dynamic quantifiable data on the enhancement of tissues before and after contrast administration. In addition to the unenhanced phase, the four-phase CT protocol at our institution includes three contrast-enhanced phases: arterial, portal, and delayed. IV contrast material was injected at 4 mL/s into an antecubital vein using a 20-gauge or larger cannula, and contrast injection was followed by a saline flush (volume = 40 mL) injected at 4 mL/s. The arterial phase was defined using a bolus-triggering technique (SmartPrep, GE Healthcare; or CARE Bolus, Siemens Healthcare): Monitoring scans were obtained 10 seconds after the start of contrast injection at 2-second intervals, and an automated triggering threshold of 175 HU at the distal thoracic aorta was used. The portal and delayed phases of scanning began 40 and 90 seconds, respectively, after completion of the arterial phase. For each phase, the scanning time for a 45-cm craniocaudal coverage ranged from 6 seconds (for the 64-MDCT scanner manufactured by GE Healthcare) to 14 seconds (for the 16-MDCT scanner manufactured by GE Healthcare). No examinations were performed with orally ingested contrast agents.

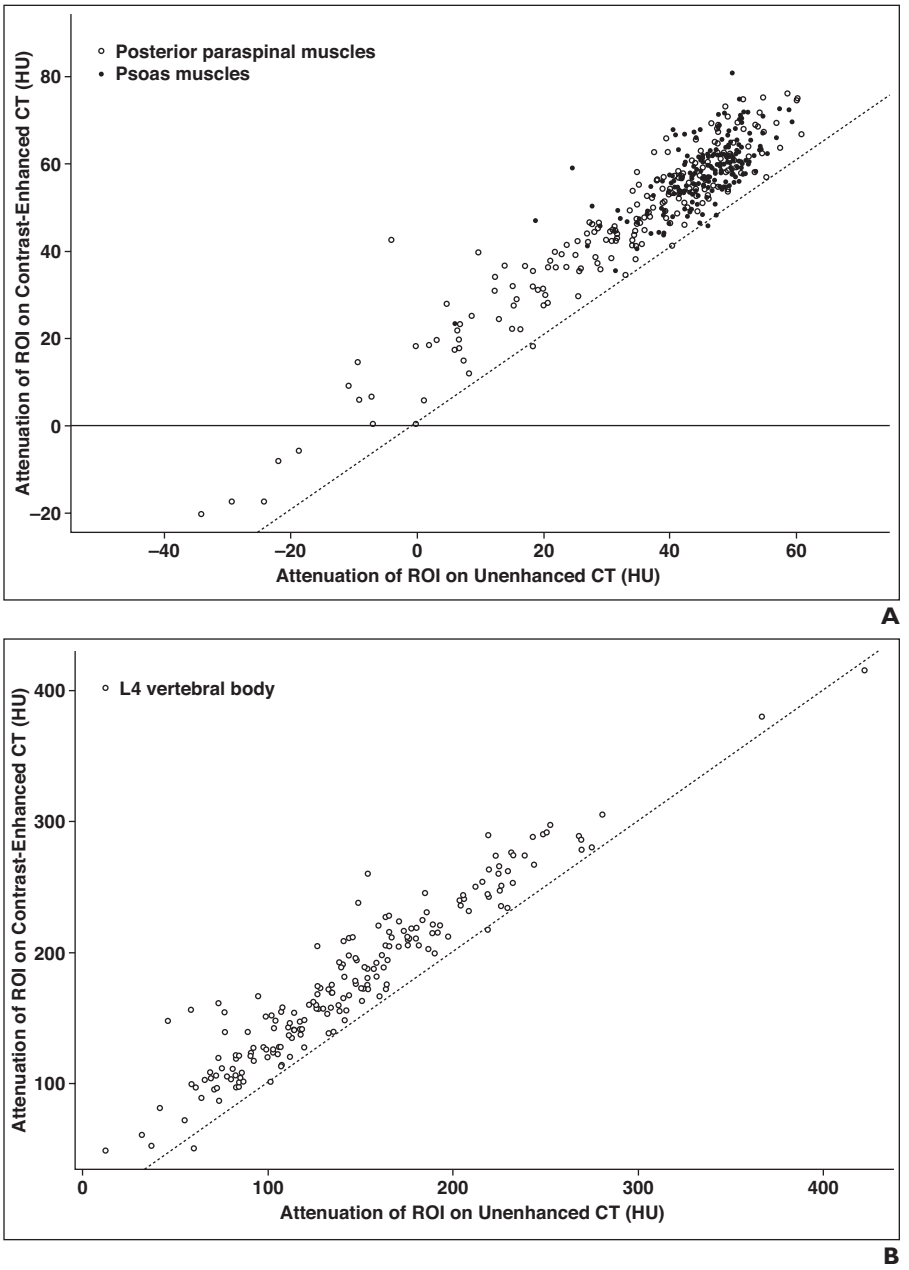

Fig. 2—Attenuation of ROIs on unenhanced CT versus contrast-enhanced CT.
A, Graph of attenuation of psoas and posterior paraspinal muscles on unenhanced CT versus contrast-enhanced CT during delayed phase. Dotted line = line of equality.
B, Graph of attenuation of L4 vertebral body on unenhanced CT versus contrast-enhanced CT during portal phase. Dotted line = line of equality.

CT Measurements

Using routine clinical PACS software (iSite, version 3.6, Philips Healthcare), two independent radiologists (one faculty radiologist with 3 years of practice after fellowship training in musculoskeletal radiology and one fellow in musculoskeletal radiology) who were blinded to clinical data performed CT measurements. The first reader independently analyzed 101 cases; the second reader independently analyzed an additional 100 cases.

TABLE 1: Patient Features and CT Findings Stratifed by Sex

Variables	All Subjects		Women		Men	
	Mean	SD	Mean	SD	Mean	SD
Patient features						
Age (y)	57.7	12.5	57.3	12.9	58.1	12.0
Body mass index[a]	28.7	6.8	29.4	7.9	28.1	5.3
CT findings						
Attenuation on unenhanced CT (HU)						
Psoas muscles	45.2	6.9	44.7	6.9	45.7	6.9
Posterior paraspinal muscles[b]	31.3	20.2	27.3	21.6	35.6	17.8
L4 vertebral body	145.2	60.7	145.5	57.9	144.9	63.9
Total psoas index[c] (cm^2/m^2)	7.2	2.6	6.1	1.8	8.3	2.8
HUAC for psoas muscles (HU)	19.7	4.5	19.4	4.1	20.1	5.0
LSAR	1.2	0.3	1.2	0.4	1.2	0.3

Note—HUAC = Hounsfield unit average calculation, LSAR = liver attenuation–to–spleen attenuation ratio.
[a]Weight in kilograms divided by the square of height in meters.
[b]Values differ significantly between women and men ($p < 0.01$).
[c]Values differ significantly between women and men ($p < 0.001$).

Joint analysis of 50 cases was performed to assess interreader variance.

Freehand ROIs were drawn on the unenhanced axial images outlining the psoas muscles at the mid L4 level, yielding cross-sectional area and attenuation measurements (Fig. 1), which were used to calculate the total psoas index (TPI) and Hounsfield unit average calculation (HUAC), two previously reported biomarkers of sarcopenia [35]. Analogous to BMI (weight in kilograms divided by the square of height in meters), the TPI is calculated to normalize the psoas area (in cm^2) for the height of the patient (in m^2) using the following equation: (right psoas area + left psoas area) / (patient $height^2$) [35]. The HUAC is a weighted average of the psoas muscle attenuation that accounts for the area of both the right and left psoas muscles [35].

Circular ROIs were placed in the right hepatic lobe (avoiding large vessels) [16] (2×1 cm^2) and the spleen (2 cm^2) to yield attenuation values on the unenhanced images; these values were used to calculate the liver attenuation–to–spleen attenuation ratio (LSAR), a marker of hepatic steatosis [36].

On all four phases, the largest circular ROI (up to 2 cm^2) accommodated by five anatomic structures was placed on axial CT images at the mid L4 level to determine the attenuation of the left and right psoas muscles, the left and right posterior paraspinal muscles, and the vertebral body cancellous bone. Circular ROI measurements for bilateral muscle regions were averaged. The L4 level was chosen because it has been validated as prognostically significant for evaluation of the body core musculature in sarcopenia patients [8, 19, 25, 37–40] and because it is commonly included in the FOV on imaging examinations of the abdomen, pelvis, and lumbar spine. Similarly, for all phases, the intraluminal attenuation of the abdominal aorta was measured with a round ROI proximal to the aortic bifurcation at the mid L3 level.

Statistical Analysis

CT attenuation and changes in attenuation after contrast administration were compared between muscle groups and between different contrast-enhanced phases of imaging with a paired *t* test. Comparisons of CT measures between groups defined by sex and clinical features were performed with a *t* test. Correlations between the CT measures were examined with the Pearson correlation coefficient (*R*).

Linear correction models were examined to assess prediction of unenhanced attenuation of tissues based on contrast-enhanced tissue attenuation. This analysis addressed the use of contrast-enhanced imaging in the absence of unenhanced imaging, which is of potential relevance to opportunistic screening. Typically contrast-enhanced imaging is acquired in only the portal or delayed phase. Therefore, linear correction models for portal and delayed imaging were performed with consideration of the patient features of age, sex, height, and weight and with consideration of aortic attenuation on contrast-enhanced imaging. Candidate prediction variables were selected on the basis of the Akaike information criterion. The prediction error for the final models was estimated using an adjusted predicted residual sum of squares (PRESS) statistic.

Interreader variance was examined with the intraclass correlation coefficient (ICC). Statistical analyses were performed using PSPP software (version 0.8.4) and R software (version 3.1.3, The R Foundation).

Results

Patients

This study evaluated 201 patients (97 men, 104 women; mean age, 57.7 ± 12.5 [SD] years; age range, 22–88 years). BMI averaged 28.7 (SD, 6.8). Common diagnoses in this cohort included obesity (73/201, 36%), diabetes (48/201, 24%), and cirrhosis (100/201, 50%).

CT Measurements

Unenhanced CT—On the unenhanced images, the mean attenuation of the psoas muscles was significantly greater than that of the posterior paraspinal muscle region (mean difference, 13.9 HU; $p < 0.001$). On unenhanced imaging, the attenuation of the posterior paraspinal muscle region (mean difference, 8.2 HU; $p < 0.01$) and the TPI (mean difference, 2.2 cm^2/m^2; $p < 0.001$) were significantly greater in men than in women (Table 1). There was, however, no significant difference between men and women in the attenuation of the psoas muscles or the HUAC. Subject age was inversely correlated with unenhanced attenuation in the psoas muscles, posterior paraspinal musculature, and L4 vertebral body ($p < 0.001$) and with the HUAC ($p < 0.001$). Subject age was also inversely correlated with the TPI in men ($p < 0.01$) but not in women (Table 2).

Contrast-enhanced CT—The psoas muscles, posterior paraspinal muscles, and L4 vertebral body enhanced significantly ($p < 0.001$) at all three contrast-enhanced phases (Table 3). For the psoas muscles and posterior paraspinal musculature, enhancement was greatest on delayed imaging, whereas enhancement in L4 was greatest in the portal phase ($p < 0.001$) (Fig. 2). The degree of enhancement in the posterior paraspinal musculature did not differ significantly from that in the psoas muscles at any of the three contrast-enhanced phases for the group ($p < 0.001$). There was significantly greater enhancement in the psoas muscles at all three contrast-enhanced phases in women than in men (arterial phase, $p < 0.05$; portal phase, $p < 0.01$; delayed phase, $p < 0.01$). There was significantly greater enhancement in the posterior paraspinal musculature in women than in men at the arterial and delayed phases ($p < 0.05$ and $p < 0.05$, respectively) but not the portal phase.

Enhancement in the psoas muscles was significantly and negatively correlated at the portal and delayed phases with the unen-

TABLE 2: Correlation of Age and Body Mass Index (BMI) With Unenhanced CT Findings Stratified by Sex

CT Findings	*R*					
	All Subjects		Women		Men	
	Age	BMI	Age	BMI	Age	BMI
Attenuation on unenhanced CT						
L4 vertebral body	−0.55[a]	0.01	−0.61[a]	0.02	−0.50[a]	0.00
Psoas muscles	−0.38[a]	−0.15[b]	−0.34[a]	−0.10	−0.43[a]	−0.21[b]
Posterior paraspinal muscles	−0.52[a]	−0.25[a]	−0.57[a]	−0.22[b]	−0.50[a]	−0.27[c]
LSAR	0.13	0.21[c]	0.09	0.28[c]	0.19	0.07
Total psoas index	−0.12	0.22[c]	0.02	0.44[a]	−0.31[c]	0.21[b]
HUAC for psoas muscles	−0.43[a]	−0.16[b]	−0.44[a]	−0.17	−0.43[a]	−0.14

Note—Values are Pearson correlation coefficients (*R*). LSAR = liver attenuation–to–spleen attenuation ratio, HUAC = Hounsfield unit average calculation.
[a]Correlation is statistically significant ($p < 0.001$).
[b]Correlation is statistically significant ($p < 0.05$).
[c]Correlation is statistically significant ($p < 0.01$).

hanced attenuation of the psoas muscles ($p < 0.05$ and $p < 0.01$, respectively) (Table 4). The TPI was significantly and negatively correlated with enhancement of the psoas muscles at all three contrast-enhanced phases (arterial phase, $p < 0.01$; portal phase, $p < 0.01$; delayed phase, $p < 0.001$) and was significantly and negatively correlated with enhancement in the posterior paraspinal muscle region on delayed phase imaging ($p < 0.01$). There was no significant correlation between enhancement in the posterior paraspinal muscle region at any phase and the unenhanced attenuation of the posterior paraspinal muscle region.

Age was positively correlated with enhancement of the paraspinal muscles at the portal and delayed phases in men ($p < 0.05$, $p < 0.01$, respectively) but not in women. This sex difference was also true of a positive age correlation with psoas enhancement in the portal phase ($p < 0.01$). Enhancement at L4 on delayed phase imaging was significantly and negatively correlated with unenhanced attenuation at L4 ($p < 0.05$) (Table 4). There were no significant sex differences in enhancement at L4. Age was positively correlated with enhancement at L4 at all contrast-enhanced phases in men (arterial phase, $p < 0.05$; portal phase, $p < 0.05$; delayed phase, $p < 0.01$) but not in women. BMI was inversely correlated with L4 enhancement at portal and delayed phases in men ($p < 0.01$, $p < 0.05$, respectively) but not in women.

Clinical Correlation With CT Measurements

Subjects with diabetes had significantly higher BMI ($p < 0.01$) and lower unenhanced attenuation in the posterior paraspinal musculature ($p < 0.05$) than nondiabetic subjects. The unenhanced attenuation of the psoas muscles, TPI, and HUAC were lower in subjects with diabetes than in nondiabetic subjects, but these differences did not reach significance. Subjects with cirrhosis had significantly lower TPI and HUAC ($p < 0.05$) than subjects without cirrhosis. In subjects with cirrhosis, MELD scores did not correlate with any of the unenhanced or contrast-enhanced CT measures.

With respect to liver steatosis, the LSAR was significantly and negatively correlated with the unenhanced attenuation of L4 and the posterior paraspinal musculature ($R = –0.18$, $R = –0.18$, respectively; $p < 0.05$) and was positively correlated with BMI ($R = 0.21$, $p < 0.01$). The LSAR was not significantly correlated with enhancement at L4, psoas muscles, or posterior paraspinal musculature at any phase and was not correlated with the unenhanced attenuation of the psoas muscles, TPI, or HUAC.

Correction Models

For the psoas muscles, variables significantly predictive of unenhanced psoas attenuation, in addition to contrast-enhanced psoas attenuation, included aortic attenuation, subject age, and subject height at both the portal and delayed phases. For the posterior paraspinal musculature, variables significantly predictive of unenhanced paraspinal muscle attenuation, in addition to contrast-enhanced paraspinal muscle attenuation, included aortic attenuation and subject age at both the portal and delayed phases. Variables predictive of unenhanced L4 attenuation, in addition to contrast-enhanced L4 attenuation, included aortic attenuation and subject age at the portal and delayed phases and patient sex at the delayed phase. These findings are summarized in Table 5. A significant intercept term was

TABLE 3: ROI Attenuation Differences Between Contrast-Enhanced CT and Unenhanced CT Stratified by Sex

CT Phase[a] and ROI	ROI Attenuation Difference Between Contrast-Enhanced CT and Unenhanced CT (HU)					
	All Subjects		Women		Men	
	Mean	SD	Mean	SD	Mean	SD
Arterial phase						
Psoas muscles[b]	4.8	5.1	5.7	6.0	3.9	3.7
Posterior paraspinal muscles[b]	4.6	4.8	5.3	4.6	3.8	4.9
L4 vertebral body	16.5	16.8	16.0	15.4	17.1	18.2
Portal phase						
Psoas muscles[c]	11.1	5.1	12.5	5.0	9.6	4.9
Posterior paraspinal muscles	11.8	6.4	12.4	6.1	11.1	6.7
L4 vertebral body	33.1	18.6	33.7	16.5	32.5	20.8
Delayed phase						
Psoas muscles[c]	12.8	5.4	14.3	5.6	11.2	4.8
Posterior paraspinal muscles[b]	13.3	5.9	14.1	5.1	12.4	6.6
L4 vertebral body	24.8	18.9	23.8	17.1	25.8	20.8

[a]Phase is the standardized period of imaging after contrast injection.
[b]Regional enhancement differs significantly between women and men ($p < 0.05$).
[c]Regional enhancement differs significantly between women and men ($p < 0.01$).

TABLE 4: Correlation of Muscle Enhancement With Unenhanced CT Features Stratified by Sex

Patient Characteristics and Unenhanced CT Features	*R* for Regional Enhancement[a]								
	Arterial Phase			Portal Phase			Delayed Phase		
	Psoas Muscles	Posterior Paraspinal Muscles	L4 Vertebral Body	Psoas Muscles	Posterior Paraspinal Muscles	L4 Vertebral Body	Psoas Muscles	Posterior Paraspinal Muscles	L4 Vertebral Body
All patients									
Age	0.03	0.02	0.06	0.12	0.05	0.08	0.02	0.12	0.13
BMI	0.08	0.09	0.01	−0.17[b]	−0.17[b]	−0.20[c]	−0.21[c]	−0.25[c]	−0.19[c]
Attenuation on unenhanced CT	−0.11	−0.08	−0.13	−0.17[b]	−0.01	−0.13	−0.23[c]	−0.07	−0.18[b]
LSAR	0.07	0.04	0.13	−0.01	−0.03	0.04	0.05	0.02	0.05
Total psoas index	−0.20[c]	−0.12	−0.11	−0.22[c]	−0.10	−0.18[b]	−0.31[d]	−0.24[c]	−0.12
HUAC for psoas muscles	0.04	0.02	0.00	−0.09	0.06	−0.01	−0.11	0.02	−0.01
Women									
Age	−0.02	−0.07	−0.13	0.02	−0.10	−0.12	−0.09	−0.02	−0.08
BMI	0.07	0.16	0.09	−0.22[b]	−0.15	−0.17	−0.22[b]	−0.22[b]	−0.15
Attenuation on unenhanced CT	−0.05	0.13	0.04	−0.14	0.12	0.01	−0.21[b]	0.06	−0.04
LSAR	0.11	0.01	0.15	−0.05	−0.13	0.01	−0.04	0.04	0.02
Total psoas index	0.06	0.13	−0.05	0.16	−0.03	−0.17	−0.14	−0.19	−0.11
HUAC for psoas muscles	0.06	0.21[b]	0.13	−0.09	0.21[b]	0.09	−0.06	0.15	0.18
Men									
Age	0.14	0.13	0.25[b]	0.28[c]	0.22[b]	0.26[b]	0.20	0.27[c]	0.32[c]
BMI	0.05	−0.04	−0.07	−0.20[b]	−0.23[b]	−0.28[c]	−0.31[c]	−0.35[d]	−0.25[b]
Attenuation on unenhanced CT	−0.18	−0.28[c]	−0.26[b]	−0.16	−0.12	−0.23[b]	−0.23[b]	−0.14	−0.29[c]
LSAR	−0.04	0.07	0.12	0.06	0.11	0.07	0.21[b]	0.00	0.09
Total psoas index	−0.41[d]	−0.14	−0.19	−0.35[c]	−0.12	−0.22[b]	−0.35[d]	−0.23[b]	−0.22[b]
HUAC for psoas muscles	0.06	−0.12	−0.10	−0.06	−0.05	−0.08	−0.13	−0.05	−0.15

Note—Values are Pearson correlation coefficients (*R*) for regional enhancement. BMI = body mass index, LSAR = liver attenuation–to–spleen attenuation ratio, HUAC = Hounsfield unit average calculation.

[a]Regional enhancement was defined as contrast-enhanced attenuation minus unenhanced attenuation.

[b]Correlation is statistically significant ($p < 0.05$).

[c]Correlation is statistically significant ($p < 0.01$).

[d]Correlation is statistically significant ($p < 0.001$).

found for the prediction of L4 unenhanced attenuation at both the portal and delayed phases and for paraspinal musculature at the delayed phase. Patient weight proved not to be significantly predictive in models when aortic attenuation was included. Aortic attenuation at all phases was negatively correlated with both height and weight ($p < 0.001$), and men were significantly heavier and taller than women ($p < 0.01$ and $p < 0.001$, respectively).

The predictive error, which was based on the adjusted residual standard error (PRESS statistic) for the psoas muscles, posterior paraspinal muscles, and L4 on delayed contrast-enhanced imaging, was 9.5% (4.3/45.2), 16.6% (5.2/31.3), and 12.6% (18.3/145.2) relative to known mean unenhanced attenuation values for these tissues, respectively.

Interreader Reliability

The ICCs for unenhanced measures of attenuation in the psoas muscles, posterior paraspinal muscles, and L4 vertebral body were 0.926, 0.677, and 0.890, respectively. Very similar ICCs were observed for each regional measure after contrast administration at all three contrast-enhanced phases: psoas muscles (0.883, 0.931, and 0.889 at arterial, portal, and delayed phases, respectively), posterior paraspinal muscles (0.675, 0.651, and 0.699 at arterial, portal, and delayed phases), and L4 (0.866, 0.888, and 0.888 at arterial, portal, and delayed phases). Although the ICCs for the psoas muscles were greater than those for the posterior paraspinal musculature at all phases, these differences did not reach significance ($p > 0.05$). The ICCs for TPI, HUAC, and LSAR were 0.960, 0.757, and 0.897, respectively.

Discussion

Although prior studies have analyzed muscle attenuation without addressing the potential effect of IV contrast administration [8, 9, 13, 19–26], we observed that significant differences do occur between the unenhanced and contrast-enhanced CT measures of muscle and bone attenuation. For both the psoas and posterior paraspinal muscles, enhancement was greatest in the delayed phase, approximately 13 HU on average, or equivalent to 28% and 43% enhancement relative to the group mean unenhanced attenuation in the psoas and posterior paraspinal musculature, respectively. Enhancement at L4

TABLE 5: Linear Correction Models for CT Enhancement in Portal and Delayed Phases

CT Feature or Patient Characteristic	Coefficient for Linear Models					
	Posterior Paraspinal Muscles		Psoas Muscles		L4 Vertebral Body	
	Portal Phase	Delayed Phase	Portal Phase	Delayed Phase	Portal Phase	Delayed Phase
Intercept	−10.31	7.78[a]	−1.70	−2.65	23.36[b]	35.65[a]
Attenuation on contrast-enhanced CT (HU)	0.88[c]	0.94[c]	0.69[c]	0.69[c]	0.92[c]	0.93[c]
Intraluminal attenuation of aorta (HU)	−0.04[a]	−0.10[c]	−0.03[a]	−0.05[c]	−0.14[c]	−0.20[a]
Age (y)	−0.11[a]	−0.10[a]	−0.09[c]	−0.06[b]	−0.32[a]	−0.37[a]
Height (m)	9.75[b]	—	10.83[a]	10.77[a]	—	—
Male[d]	—	—	—	—	—	−3.89
Residual SE	5.71	5.12	3.91	4.26	17.54	18.06
Adjusted residual SE[e]	5.80	5.18	3.99	4.34	17.87	18.29
R^2	0.92	0.93	0.68	0.62	0.92	0.91

Note—Prediction error for final models was estimated using an adjusted predicted residual sum of squares (PRESS) statistic. Dash (—) indicates that the variable does not have predictive value in the linear model. SE = standard error, R^2 = coefficient of determination. Values represent coefficients for linear models that estimate unenhanced tissue attenuation based on contrast-enhanced tissue attenuation and other selected patient features.

[a]Significance level for coefficient is $p < 0.01$.
[b]Significance level for coefficient is $p < 0.05$.
[c]Significance level for coefficient is $p < 0.001$.
[d]The variable "male" equals 1 for men and 0 for women.
[e]Based on PRESS statistic.

was also substantial and was greatest in the portal phase, approximately 33 HU on average, equivalent to 23% enhancement relative to the group mean unenhanced attenuation at L4. We are not aware of any prior studies evaluating the enhancement of muscle and bone with four-phase CT.

For both muscle and bone in our study, patient age was highly correlated with decreased unenhanced CT attenuation, which is consistent with the work of others [2, 41]. The HUAC, a proposed biomarker of sarcopenia, was also inversely correlated with patient age.

Muscle

We observed a significantly lower attenuation of the posterior paraspinal musculature in women than men, but we did not observe a significant difference between men and women in the unenhanced attenuation of the psoas muscles. This result is in line with prior work [42] that has shown no difference in psoas muscle attenuation for older men versus older women, despite the significantly lower attenuation of the posterior paraspinal muscles in women compared with men. Previous research has shown that posterior paraspinal muscles are composed primarily of type I (slow-twitch) fibers, whereas the psoas muscles are composed of a higher proportion of type II (fast-twitch) fibers [43]. Type I muscle has lower glycolytic capacity than type II muscle [43], has greater lipid content than type II muscle [44], and reportedly may undergo preferential atrophy with disuse [45]. Specific mechanisms responsible for sex differences and regional variations in muscle metabolism are active areas of research [44].

We also observed other significant sex-based differences in muscle. First, although the TPI (i.e., cross-sectional area of the psoas muscle normalized for patient height) decreased with age in men, no significant correlation of TPI with age was observed in women. Second, significant positive correlations between age and muscle enhancement were observed in men but not in women. Finally, contrast enhancement in both the psoas and posterior paraspinal muscles was significantly greater in women than men. This difference, however, may simply reflect the use of a standard dose of contrast material (125 mL) that was not adjusted for body weight; men were significantly heavier and taller than women in this study.

Increased lipid concentrations in muscle are associated with lower CT attenuation measurements. Specifically, an increase in lipid concentration of 1 g per 100 mL results in a decrease in CT attenuation of approximately 1 HU [7]. A proposed muscle attenuation threshold for diagnosing myosteatosis on CT is 30 HU [13, 41]; other defining cut points for myosteatosis have also been used [13, 23]. The influences of numerous clinical conditions on muscle attenuation have been documented, and decreases on the order of 3–6 HU have been reported for each of the following factors: subjects who are female, obese, diabetic (type II), and deconditioned and those who have the common orthopedic problems of hip osteoarthritis and low back pain [41]. The magnitude of muscle attenuation change related to IV contrast material that we observed in our study—a mean of 4–13 HU depending on the contrast-enhanced phase—appears substantial relative to muscle attenuation changes ascribed with prognostic significance in previous studies of sarcopenia and myosteatosis.

Although hepatic steatosis or nonalcoholic fatty liver disease has been linked to sarcopenia in prior studies [16, 17], we did not observe a correlation between the LSAR (the marker of hepatic steatosis used in our study) and the TPI or HUAC in our study group. The LSAR also was not significantly correlated with enhancement at L4, psoas muscles, or posterior paraspinal musculature at any phase.

Bone

We found that unenhanced attenuation at L4 was negatively correlated with enhancement on delayed phase imaging, whereas BMI was negatively correlated with enhancement at both the portal and delayed phases. There were no significant sex differences in cancellous bone enhancement at L4.

The magnitude of contrast-related change in L4 attenuation—as high as 33.1 HU (group mean) in the portal phase—would substantially alter the interpretation of CT attenuation measures as markers of cancellous bone mineral density. Our findings are consistent with those of others [28, 29, 46] who also found cancellous bone marrow enhancement on contrast-enhanced (predominantly portal phase) CT of the lumbar spine. For example, investigators reported that enhancement of up to 25 HU at the L1 vertebral body was observed in 73% of patients and that enhancement of more than 25 HU was observed in 27% of patients (mean increase of 11 HU, or ≈ 8%) [29]. By correlating their results with dual-energy x-ray absorptiometry, these authors [29] concluded that L1 attenuation thresholds for diagnosing osteoporosis with 90% specificity were

90 and 102 HU on unenhanced and contrast-enhanced CT examinations, respectively. Other investigators [28] concluded that contrast-enhanced CT can lead to underestimation of osteoporosis compared with unenhanced CT in 7–25% of patients. When a 130-HU threshold at L3 was used for the diagnosis of osteoporosis, as established by other investigators [47], the diagnosis of osteoporosis based on unenhanced imaging would have changed in 22%, 37%, and 32% of our patients (false-negative rates of 25%, 43%, and 37%) using contrast-enhanced CT at the arterial, portal, and delayed phases, respectively.

The results of our study must be interpreted in light of limitations. First, the attenuation numbers produced by CT are affected by numerous technical and patient factors. We attempted to minimize the variability of these factors by using a single CT protocol and standardizing the tube voltage, contrast volume, contrast concentration, and contrast injection rate. Second, manual attenuation measurements are subject to interobserver and intraobserver variability, although reliability has been shown to be good to excellent among trained observers [23, 28]. To address this potential concern, we analyzed interreader agreement and found it to be strong. Third, the subjects in this study were generally older adult patients with medical problems (i.e., not young, asymptomatic subjects). This population is typical of groups for whom sarcopenia and osteoporosis are of practical and clinical importance, and we made this cohort selection intentionally.

In summary, our study documents the extent to which IV contrast injection alters the CT attenuation of commonly measured skeletal muscle and vertebral cancellous bone regions during the arterial, portal, and delayed phases. Indeed, for both bone and muscle, contrast administration and the timing of subsequent CT can significantly change the attenuation values that are used as biomarkers for sarcopenia and osteoporosis. Our study also indicates that contrast enhancement may vary significantly with age, sex, and unenhanced tissue attenuation and, in the case of muscle, by anatomic region. Substantial intersubject variation in contrast enhancement appears to limit simple correction of contrast-enhanced muscle and bone attenuation when only contrast-enhanced imaging is acquired even with a highly standardized injection and CT protocol.

References

1. Pickhardt PJ, Pooler BD, Lauder T, del Rio AM, Bruce RJ, Binkley N. Opportunistic screening for osteoporosis using abdominal computed tomography scans obtained for other indications. *Ann Intern Med* 2013; 158:588–595
2. Lee S, Chung CK, Oh SH, et al. Correlation between bone mineral density measured by dual-energy X-ray absorptiometry and Hounsfield units measured by diagnostic CT in lumbar spine. *J Korean Neurosurg Soc* 2013; 54:384–389
3. Fidler JL, Murthy NS, Khosla S, et al. Comprehensive assessment of osteoporosis and bone fragility with CT colonography. *Radiology* 2016; 278:172–180
4. Schreiber JJ, Gausden EB, Anderson PA, et al. Opportunistic osteoporosis screening: gleaning additional information from diagnostic wrist CT scans. *J Bone Joint Surg Am* 2015; 97:1095–1100
5. Boutin RD, Yao L, Canter RJ, Lenchik L. Sarcopenia: current concepts and imaging implications. *AJR* 2015; 205:[web]W255–W266
6. Gomez-Perez SL, Haus JM, Sheean P, et al. Measuring abdominal circumference and skeletal muscle from a single cross-sectional computed tomography image: a step-by-step guide for clinicians using National Institutes of Health ImageJ. *J Parenter Enteral Nutr* 2016; 40:308–318
7. Goodpaster BH, Kelley DE, Thaete FL, He J, Ross R. Skeletal muscle attenuation determined by computed tomography is associated with skeletal muscle lipid content. *J Appl Physiol (1985)* 2000; 89:104–110
8. Sabel MS, Lee J, Cai S, Englesbe MJ, Holcombe S, Wang S. Sarcopenia as a prognostic factor among patients with stage III melanoma. *Ann Surg Oncol* 2011; 18:3579–3585
9. Miller BS, Ignatoski KM, Daignault S, et al. Worsening central sarcopenia and increasing intra-abdominal fat correlate with decreased survival in patients with adrenocortical carcinoma. *World J Surg* 2012; 36:1509–1516
10. Miljkovic I, Kuipers AL, Cauley JA, et al. Greater skeletal muscle fat infiltration is associated with higher all-cause and cardiovascular mortality in older men. *J Gerontol A Biol Sci Med Sci* 2015; 70:1133–1140
11. Montano-Loza AJ, Angulo P, Meza-Junco J, et al. Sarcopenic obesity and myosteatosis are associated with higher mortality in patients with cirrhosis. *J Cachexia Sarcopenia Muscle* 2015; 7:126–135
12. Fujiwara N, Nakagawa H, Kudo Y, et al. Sarcopenia, intramuscular fat deposition, and visceral adiposity independently predict the outcomes of hepatocellular carcinoma. *J Hepatol* 2015; 63:131–140
13. Rollins KE, Tewari N, Ackner A, et al. The impact of sarcopenia and myosteatosis on outcomes of unresectable pancreatic cancer or distal cholangiocarcinoma. *Clin Nutr* 2015 Sep 1 [Epub ahead of print]
14. Schnyder S, Handschin C. Skeletal muscle as an endocrine organ: PGC-1α, myokines and exercise. *Bone* 2015; 80:115–125
15. Bouillon R, Drucker DJ, Ferrannini E, Grinspoon S, Rosen CJ, Zimmet P. The past 10 years: new hormones, new functions, new endocrine organs. *Nat Rev Endocrinol* 2015; 11:681–686
16. Hong HC, Hwang SY, Choi HY, et al. Relationship between sarcopenia and nonalcoholic fatty liver disease: the Korean Sarcopenic Obesity Study. *Hepatology* 2014; 59:1772–1778
17. Poggiogalle E, Lubrano C, Gnessi L, Mariani S, Lenzi A, Donini LM. Fatty liver index associates with relative sarcopenia and GH/IGF-1 status in obese subjects. *PLoS One* 2016; 11:e0145811
18. Buch A, Carmeli E, Boker LK, et al. Muscle function and fat content in relation to sarcopenia, obesity and frailty of old age: an overview. *Exp Gerontol* 2016; 76:25–32
19. Englesbe MJ, Lee JS, He K, et al. Analytic morphomics, core muscle size, and surgical outcomes. *Ann Surg* 2012; 256:255–261
20. Waits SA, Kim EK, Terjimanian MN, et al. Morphometric age and mortality after liver transplant. *JAMA Surg* 2014; 149:335–340
21. Prado CM, Lieffers JR, McCargar LJ, et al. Prevalence and clinical implications of sarcopenic obesity in patients with solid tumours of the respiratory and gastrointestinal tracts: a population-based study. *Lancet Oncol* 2008; 9:629–635
22. Antoun S, Lanoy E, Iacovelli R, et al. Skeletal muscle density predicts prognosis in patients with metastatic renal cell carcinoma treated with targeted therapies. *Cancer* 2013; 119:3377–3384
23. Martin L, Birdsell L, Macdonald N, et al. Cancer cachexia in the age of obesity: skeletal muscle depletion is a powerful prognostic factor, independent of body mass index. *J Clin Oncol* 2013; 31:1539–1547
24. Chu MP, Lieffers J, Ghosh S, et al. Skeletal muscle radio-density is an independent predictor of response and outcomes in follicular lymphoma treated with chemoimmunotherapy. *PLoS One* 2015; 10:e0127589
25. Kirk PS, Friedman JF, Cron DC, et al. One-year postoperative resource utilization in sarcopenic patients. *J Surg Res* 2015; 199:51–55
26. Malietzis G, Johns N, Al-Hassi HO, et al. Low muscularity and myosteatosis is related to the host systemic inflammatory response in patients undergoing surgery for colorectal cancer. *Ann Surg* 2016; 263:320–325
27. Bauer JS, Henning TD, Müeller D, Lu Y, Majumdar S, Link TM. Volumetric quantitative CT of the spine and hip derived from contrast-enhanced MDCT: conversion factors. *AJR* 2007; 188:1294–1301
28. Pompe E, Willemink MJ, Dijkhuis GR, Verhaar

HJ, Mohamed Hoesein FA, de Jong PA. Intravenous contrast injection significantly affects bone mineral density measured on CT. *Eur Radiol* 2015; 25:283–289

29. Pickhardt PJ, Lauder T, Pooler BD, et al. Effect of IV contrast on lumbar trabecular attenuation at routine abdominal CT: correlation with DXA and implications for opportunistic osteoporosis screening. *Osteoporos Int* 2016; 27:147–152
30. Ziemlewicz TJ, Maciejewski A, Binkley N, Brett AD, Brown JK, Pickhardt PJ. Direct comparison of unenhanced and contrast-enhanced CT for opportunistic proximal femur bone mineral density measurement: implications for osteoporosis screening. *AJR* 2016; 206:694–698
31. Engelke K, Lang T, Khosla S, et al. Clinical use of quantitative computed tomography–based advanced techniques in the management of osteoporosis in adults: the 2015 ISCD Official Positions. Part III. *J Clin Densitom* 2015; 18:393–407
32. Wilmink JT, Roukema JG. Effects of IV contrast administration on intraspinal and paraspinal tissues: a CT study. Part 1. Measurement of CT attenuation numbers. *AJNR* 1987; 8:703–709
33. Runge VM, Marquez H, Andreisek G, Valavanis A, Alkadhi H. Recent technological advances in computed tomography and the clinical impact therein. *Invest Radiol* 2015; 50:119–127
34. Brix G, Bahner ML, Hoffmann U, Horvath A, Schreiber W. Regional blood flow, capillary permeability, and compartmental volumes: measurement with dynamic CT—initial experience. *Radiology* 1999; 210:269–276
35. Joglekar S, Asghar A, Mott SL, et al. Sarcopenia is an independent predictor of complications following pancreatectomy for adenocarcinoma. *J Surg Oncol* 2015; 111:771–775
36. Zeb I, Li D, Nasir K, Katz R, Larijani VN, Budoff MJ. Computed tomography scans in the evaluation of fatty liver disease in a population based study: the multi-ethnic study of atherosclerosis. *Acad Radiol* 2012; 19:811–818
37. Lee JS, He K, Harbaugh CM, et al. Frailty, core muscle size, and mortality in patients undergoing open abdominal aortic aneurysm repair. *J Vasc Surg* 2011; 534:912–917
38. Krell RW, Kaul DR, Martin AR, et al. Association between sarcopenia and the risk of serious infection among adults undergoing liver transplantation. *Liver Transpl* 2013; 19:1396–1402
39. Sheetz KH, Zhao L, Holcombe SA, et al. Decreased core muscle size is associated with worse patient survival following esophagectomy for cancer. *Dis Esophagus* 2013; 26:716–722
40. Zarinsefat A, Terjimanian MN, Sheetz KH, et al. Perioperative changes in trunk musculature and postoperative outcomes. *J Surg Res* 2014; 191:106–112
41. Aubrey J, Esfandiari N, Baracos VE, et al. Measurement of skeletal muscle radiation attenuation and basis of its biological variation. *Acta Physiol (Oxf)* 2014; 210:489–497
42. Anderson DE, D'Agostino JM, Bruno AG, Demissie S, Kiel DP, Bouxsein ML. Variations of CT-based trunk muscle attenuation by age, sex, and specific muscle. *J Gerontol A Biol Sci Med Sci* 2013; 68:317–323
43. Regev GJ, Kim CW, Thacker BE, et al. Regional myosin heavy chain distribution in selected paraspinal muscles. *Spine* 2010; 35:1265–1270
44. Schiaffino S, Reggiani C. Fiber types in mammalian skeletal muscles. *Physiol Rev* 2011; 91:1447–1531
45. Ciciliot S, Rossi AC, Dyar KA, Blaauw B, Schiaffino S. Muscle type and fiber type specificity in muscle wasting. *Int J Biochem Cell Biol* 2013; 45:2191–2199
46. Acu K, Scheel M, Issever AS. Time dependency of bone density estimation from computed tomography with intravenous contrast agent administration. *Osteoporos Int* 2014; 25:535–542
47. Pickhardt PJ, Lee LJ, del Rio AM, et al. Simultaneous screening for osteoporosis at CT colonography: bone mineral density assessment using MDCT attenuation techniques compared with the DXA reference standard. *J Bone Miner Res* 2011; 26:2194–2203

FOR YOUR INFORMATION

This article is available for CME and Self-Assessment (SA-CME) credit that satisfies Part II requirements for maintenance of certification (MOC). To access the examination for this article, follow the prompts associated with the online version of the article.